

A GEOPHYSICAL ASSESSMENT FOR ENGINEERING PERFORMANCE OF SUBGRADE SOILS: A CASE STUDY OF THE AGO-IWOYE/ILISHAN ROAD, SOUTH- WESTERN NIGERIA.

Olufemi, S.T.¹, Adekoya, S.A.², Ariyo, S. O.,¹Adebisi, N.O.,¹ Coker, J.O.² and Aguiyi, D.P.O.³

¹*Department of Earth Sciences, Olabisi Onabanjo University, Ago-Iwoye, Ogun State*

²*Department of Physics, Olabisi Onabanjo University, Ago-Iwoye, Ogun State*

³*Independent Consultants Nigeria (ICN), Port Harcourt Rivers State*

Email: olufemi.sunday@oouagoiwoye.edu.ng ; adebisi.niyi@oouagoiwoye.edu.ng

Corresponding Authors: coker.joseph@oouagoiwoye.edu.ng

adekoya.sofiat@oouagoiwoye.edu.ng; daguiyi@yahoo.com

Received: 04-10-2023

Accepted: 14-11-2023

<https://dx.doi.org/10.4314/sa.v23i1.2>

This is an Open Access article distributed under the terms of the Creative Commons Licenses [CC BY-NC-ND 4.0]

<http://creativecommons.org/licenses/by-nc-nd/4.0>.

Journal Homepage: <http://www.scientia-african.uniportjournal.info>

Publisher: *Faculty of Science, University of Port Harcourt.*

ABSTRACT

Geophysical application of electrical resistivity method has been employed to differentiate subsurface target of interest from the encompassing strata along the Ago-Iwoye/Ilishan road in South-western Nigeria. However, a geological model which links variation in lithological characteristics of subgrade soils to the engineering performance of the road is yet to be a research subject. This research is a special geotechnical application of geophysics for revealing the subsurface disposition and predicting the stability state of subgrade materials. Field assessment of rock types, and their relationship was followed by electrical resistivity measurement along the road. Schlumberger and dipole – dipole arrays were adopted for fifty-eight (58) Vertical Electrical Sounding (VES) and 2-D resistivity imaging involving Dipole-Dipole profiling technique was adopted in the sedimentary segment. Field data were inverted to 2-D resistivity structures inferentially delineated contour colorations using ‘DIPRO for Windows’ software. Geo-electric layers revealed Sedimentary Basin (SB) between Ilishan and Irolu, between Irolu and Ijesha-Ijebu, Transitional Zone (TZ) with abrupt contrast along the plane of an unconformity and crystalline Basement Complex (BC) towards Ago-Iwoye. The 2-D resistivity structures across the different geological terrains revealed with 50Ωm - 3289Ωm at SB, 233Ωm - 8028Ωm at TZ and 8Ωm - 3009Ωm at BC. From geotechnical view, subgrade materials underlying the SB and TZ segments can be adjudged competent to sand and clayey sand units with minor occurrences of incompetent clay and sandy clay lenses. The occurrence of subsurface discontinuities at the BC end of TZ of the road would adversely affect the pavement stability.

Keywords: Resistivity, Geotechnical, Subgrade, 2-D and Road

INTRODUCTION

The Ago-Iwoye/Ilishan road in the tropical, South-western part of Nigeria, has been unstable and is experiencing different levels of

failures at different locations. The road links major roads, from the South-western Nigeria to other major cities across the nation. Presently, the road is undergoing upgrading and rehabilitation. Adebisi and Fatoba (2013)

identified cost and difficulty of recovering geotechnical samples to obtain satisfactory results for site investigation. For this particular reason, *in-situ* acquisition was recommended for accurate geotechnical information acquisition on the nature of subsurface conditions prior to construction project. Geophysical survey for roads/highways subgrade soils is performed on the ground surface. This is because methods of obtaining both disturbed and undisturbed samples, boring as well as direct physical *in-situ* geotechnical testing are destructive, and make results of tests doubtful in predicting the actual ground condition (TRC, 2008). The electrical resistivity method of geophysics is a non-destructive testing (NDT) tool, which measures specific parameters that can be used to generate physical property models (Anderson, 2006; Anderson *et al.*, 2008; Martinho and Dionísio, 2014; Coe *et al.*, 2017; Capozzoli and Rizzo, 2017).

The application of geophysics to engineering investigations normally extend to a considerable depth within the subsurface (Wightman *et al.*, 2004; Hoover, 2004). According to Olorunfemi *et al.*, (2004) the electrical resistivity method is a rapid means of obtaining information regarding foundation condition of structure. It is non-destructive compared to direct geotechnical method of sampling (Sirles, 2006). Electrical resistivity survey method has been widely employed for well-planned, cost-effective drilling and testing programs, and has provided reliable volumetric image of the the nature and variability of the subsurface between existing boreholes (Hempfen *et al.*, 2000; Olayinka and Oyedele, 2001).

In this study, it is thoughtful that geologic models would present precise illustrations of relatively, small-scale variations in the nature of the subgrade soils from their encompassing

sedimentary and crystalline parent rocks. The spatial resistivity variations of two different bedrock systems that had undergone physical weathering, and had been chemically transformed into soils over the geologic time were electrically measured. These soils serve as (foundation materials) subgrade for the Ago-Iwoye/Ilishan road. This is expected to draw inferences on the differences in the ability of the flexible road pavement to resist wheel load over the subgrade soils. On the basis of contrasting lithological characteristics, the output geologic models would reveal the basis for different levels of failures at different locations. This will serve as an essential utility for the engineers who are in responsible charge of designing the highway under rehabilitation.

Physical Disposition and Geological Settings

The area under study cuts across Ilishan and Ago-Iwoye between longitudes 3.7-3.92° E and latitudes 6.86-6.98° N in Southwestern Nigeria. Many research works including Akanni (1992) have discussed the physical setting of the area. The main target for this study is the road that links Ilishan with Ago-Iwoye. The Ilishan and Ago-Iwoye road covers a considerable distance of about 25km, and it is easily accessible (Figure 1). Nature and types of vegetation cover is typical of the tropical climate areas, where alternating wet and dry seasons are being experienced. Its drainage pattern is virtually dendritic, and controlled by contrasting topographical setting of the area.

The residual laterized soils in such an area forms the profile of varying thicknesses over two genetically different bedrocks (Scalenghe *et al.*, 2016). The first is the sedimentary strata of the Dahomey Basin, and the other is the Migmatite-Gneiss complex of the Precambrian Basement rocks. The Ago-

Iwoye/Ilishan road is a highway and it cuts across this location of two distinct geological zones. Thus, the road is underlain by rocks of drastically different composition.

From Ilishan to Ijesha-Ijebu, the road is underlain by the Neocomian-Albian Ise Formation of the Abeokuta Group. The Abeokuta Group comprises the Ise, Afowo and Araromi Formation (Oli *et al.*, 2019). The Ise Formation is virtually exposed unconformably at Ijesha-Ijebu, and overlies the crystalline Basement Complex rocks. This Formation consists of ferruginised conglomeratic, grits, coarse to medium grained-sized sands that are interbedded with kaolinite (NGSA, 2006).

Rocks of the Gneiss complex underlain the Ago-Iwoye to Ijesha-Ijebu part of the study area. Few outcrops are available for mapping in the area. Bayewu *et al.*, (2011) reported pegmatite, granite gneiss, banded gneiss and migmatite gneiss as the major rock types in the area. Balogun (2019) discussed the geologic setting and structural disposition of the Nigerian Basement Complex rocks. It is noted to comprise suites of Granitic bodies (porphyritic granite, medium/coarse-grained biotite granite, hornblende granite, granodiorite and granite gneiss) intruded the Migmatite–Gneiss–Quartzite Complex of Precambrian to Cambrian age. These rocks are of Pan-African age across Nigeria.

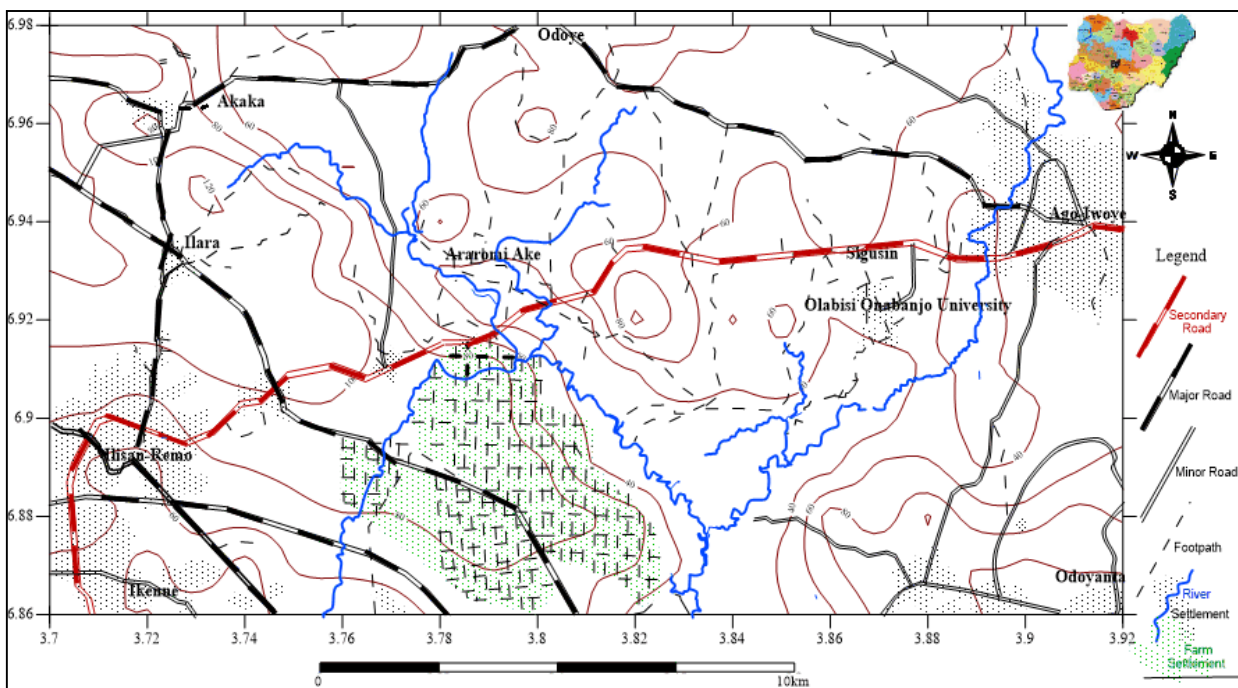


Figure 1. Map of the physiographic features of the study area

METHOD OF STUDY

This research commenced with a reconnaissance survey for field assessment of the rock types, and how they were related. This was followed by geophysical survey by electrical resistivity measurement along the road covering two distinct geological zones including where both the sedimentary

Formation and the basement complex crystalline rocks overlap. The reconnaissance was done across the entire stretch of the road for rapid tracking of existing and newly adjoined accessibility. The field stage encompassed reconnaissance inspection, topographic update and confirmation of outcrops from the existing geological map.

The sounding stations were strategically positioned along the investigated route (Figure 2) to starkly, reveal its lithologic settings. This is consistent with method of geophysical acquisition for lateral variations in the nature of the bedrocks (Anderson, 2006; Anderson *et al.*, 2008). Schlumberger and dipole – dipole arrays were adopted for vertical electrical sounding (VES) and electrical resistivity imaging (ERI) of the subsurface respectively. A total of twelve (12) dipole-dipole ground electrical resistivity surveys were carried out in the area (5 at the basement complex area, 2 at the basement-sedimentary interface and 5 in the sedimentary terrain.

Furthermore, fifty-eight (58) Vertical Electrical Soundings (VES) were also carried out from the Basement area, through the

basement-sedimentary interface to the sedimentary terrain.

2-D resistivity imaging involving Dipole-Dipole profiling technique was adopted in the sedimentary segment of the road to map the vertical discontinuities typical of jointed, fractured and faulted zones (Karous and Hjelt *et al.*, 1983). The field data were inverted to 2-D resistivity structure using ‘DIPRO for Windows’ software. Lithologic variations depicted on the 2-D inverted resistivity structures were inferentially delineated with the aid of the resistivity contour colorations, but the interpretations assigned to a colouration depends on the observed electrical resistivity distribution on the structure. This is generally uneven within the probed subgrade due to its varied lithologic composition.

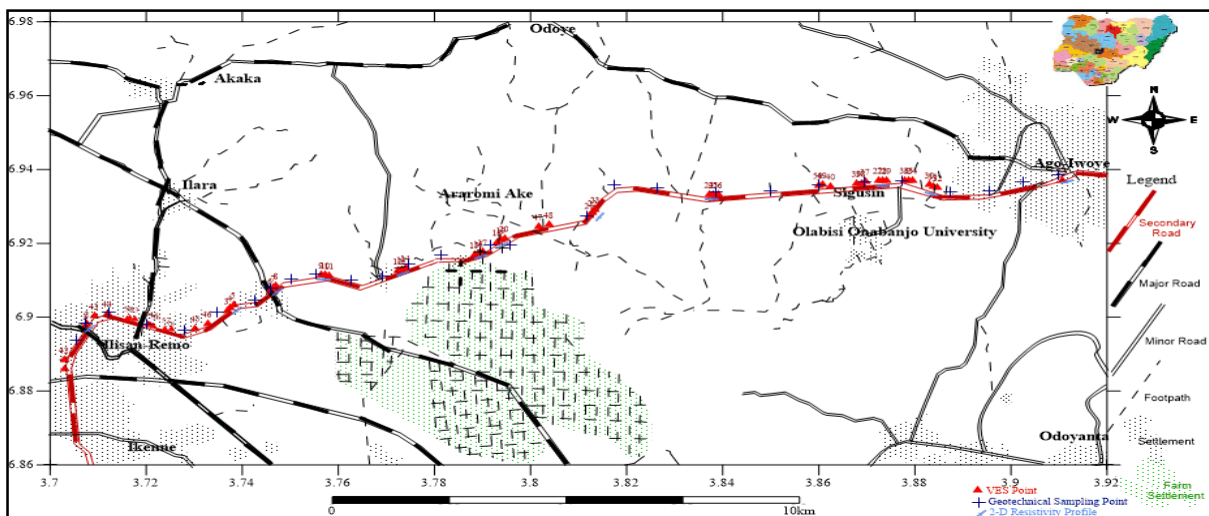


Figure 2. Modified geological map of the study area (After NGS, 2006)

DISCUSSION OF RESULTS

Geoelectric Parameters

The fifty-eight (58) Vertical Electrical Sounding (VES) iterated curves and the field data were interpreted. Although, the curves are inconsistent in shape over the three geologic conditions (sedimentary basin, transition and basement complex) however, their shape around the origin is largely of the ‘bowl’ type. This is in most cases portrays four (4) geo-

electric layers. The abridged result of the vertical electrical sounding data acquired along the sedimentary section of the investigated road is shown in Table 1. It reveals a range of three to five geo-electric layers, from topsoil to the bedrock. The electrical resistivity ranges are 73-1606 Ω m, 1340 Ω m, 65-96 Ω m/101 –192 Ω m/215-582 Ω m, 621-7405 Ω m and 526-1919 Ω m.

These depict topsoil, laterite, hybrid clastic sediment (clay/sandy clay/clayey sand), dry sand and sandstone. Thickness ranges from the topsoil top the underlying hybrid stratum is 0.6m -1.9m and 1.8m – 3.8m/4.0m – 9.8m/1.9m – 4.4m in that order; and at determinable points, the thickness of the sand stratum ranges between 37.3m to 47.6m but undeterminable for the deepest encountered wet sandstones. In view of the targeted shallow

occurrence of the probed layers, greater emphasis is laid on the electrical resistivity property of the subgrade layer on the road. With the exception of the lowly electrically resistive clayey, topsoil delineated along an unpaved section at Ilishan, the resistivity of the top soil is considerably high enough and it is of indicative competent pavement support towards the sedimentary-basement transition zone.

Table 1. Abridged VES Results over the Sedimentary Terrain

VES NO	LAYER NUMBER	RESISTIVITY (Ω m)	THICKNESS (m)	DEPTH (m)	CURVE TYPE	INFERRED LITHOLOGY
1	1	95.0	1.0	1.0	A	Topsoil
	2	101.0	4.0	5.0		Sandy Clay
	3	855.0	---	---		Sand
2	1	73.1	1.9	1.9	A	Topsoil
	2	191.7	4.7	6.6		Sandy Clay
	3	621.4	---	---		Sand
3	1	312.5	0.6	0.6	HA	Topsoil
	2	110.5	1.7	2.3		Sandy Clay
	3	156.7	8.1	10.4		Sandy Clay
	4	2404.5	---	---		Dry Sand
8	1	638.7	0.7	0.7	H	Topsoil
	2	77.8	2.1	2.8		Clay
	3	3897.4	---	---		Dry Sand
9	1	375.7	1.1	1.1	HK	Topsoil
	2	243.7	1.9	3.0		Clayey Sand
	3	1584.6	47.6	50.6		Dry Sand
	4	526.9	---	---		Wet Sandstone
10	1	1317.2	1.1	1.1	H	Topsoil
	2	386.3	4.0	5.1		Clayey Sand
	3	4932.6	---	---		Dry Sand
14	1	1075.2	0.8	0.8	KHK	Topsoil
	2	1339.9	0.8	1.6		Laterite
	3	582.3	2.6	4.2		Clayey Sand
	4	7405.2	37.3	41.5		Dry Sand
	5	1919.2	---	---		Wet Sandstone
41	1	34.2	1.2	1.2	A	Topsoil
	2	44.8	3.8	5.0		Clay
	3	783.1	-	-		Sand
42	1	421.1	0.9	0.9		Topsoil

	2	42.3	6.0	6.9	H	Clay
	3	1541.8	-	-		Sand
43	1	390	0.7	0.7	KH	Topsoil
	2	490	4.8	5.5		Clayey Sand
	3	90	19.5	25		Clay
	4	4500	-	-		Dry Sand
44	1	487.8	1.2	1.2	QH	Topsoil
	2	312.4	6.5	7.7		Clayey Sand
	3	96.8	23.2	30.9		Clay
	4	876.5	-	-		Sand
45	1	157.3	0.6	0.6	HA	Topsoil
	2	75.1	1.3	1.9		Clay
	3	1528.7	5.1	7.0		Sand
	4	12534.2	-	-		Dry Sand
46	1	99.6	1.2	1.2	A	Topsoil
	2	184.8	1.1	2.3		Sandy Clay
	3	46264.7	-	-		Dry Sand
47	1	105.3	2.2	2.2	A	Topsoil
	2	527.3	15.4	17.7		Sand
	3	6633.7	-	-		Dry Sand
54	1	141.1	0.6	0.6	A	Topsoil
	2	1154.4	10.2	10.8		Sand
	3	4865.6	-	-		Dry Sand
55	1	131.0	1.2	1.2	A	Topsoil
	2	990.6	11.8	13.0		Sand
	3	3098	-	-		Dry Sand
56	1	101.7	2.2	2.2	A	Topsoil
	2	320.4	7.9	10.1		Clayey Sand
	3	1729.5	-	-		Sand
57	1	269.1	1.1	1.1	A	Topsoil
	2	848.5	8.0	9.1		Sand
	3	3460.7	-	-		Dry Sand
58	1	253.6	1.0	1.0	A	Topsoil
	2	1017.8	8.3	9.4		Sand
	3	2885.1	-	-		Dry Sand

At the transition zone (Sedimentary-Basement interface), the road segment, the geo-electric section depicts lithologic transitions from sedimentary to basement boundary (Table 2). Along the sedimentary margin, there is anomalously high electrical resistivity, which marks the termination of the sedimentary environment. There exists a five geo-electric stratum with electrical resistivity values of 6965 Ω m, 9622 Ω m, 2043 Ω m, and 5514 Ω m and 851 Ω m. These were from topmost to the bedrock as topsoil, ferruginous conglomeratic sand, ferruginous sand, and conglomeratic sandstone.

An abrupt contrast in resistivity was evident along the plane of an unconformity between the two terrains. On the basement flank of the traverse, there exist five (5) geo-electric layers with respective

resistivity ranges of 871 – 2137 Ω m (topsoil), 668 – 1407 Ω m (sand), 48 Ω m (kaolinitic clay), 238 - 381 Ω m (clayey sand) and 5039 - 6888 Ω m (basement) were delineated from top to basement rock.

Table 2. VES Results over the (Sedimentary-Basement interface) Transition Zone

VES NO	LAYER NUMBER	RESISTIVITY (Ω m)	THICKNESS (m)	DEPTH (m)	CURVE TYPE	INFERRED LITHOLOGY
15	1	6964.9	0.8	0.8	KHK	Topsoil
	2	9621.7	3.1	3.9		Conglomeratic Sand
	3	2042.5	22.4	26.3		Dry Sand
	4	5513.7	20.8	47.2		Conglomeratic Sand Sandstone
	5	851.3	---	---		Sand
16	1	2135.0	2.2	2.2	HKH	Topsoil
	2	667.7	6.9	9.1		Sand
	3	1407.2	9.3	18.4		Sand
	4	381.3	17.1	35.5		Clayey Sand
	5	5039	---	---		Fresh Basement
17	1	870.8	1.1	1.1	HA	Topsoil
	2	47.7	15.1	16.2		Clay
	3	238.3	8.3	24.4		Clayey Sand
	4	6887.5	---	---		Fresh Basement

From Table 3, it is obvious that a range of three (3) to five (5) geo-electric layers is also peculiar to the Basement Complex segment of the road. Lithologic inferences drawn from the mapped layers delineated three main lithologic units. The electrical resistivity ranges are 12 - 1063 Ω m (topsoil), 36 - 1257 Ω m (capped or uncapped heterogeneous weathered unit) and 457 - 3892 Ω m (the fractured/fresh bedrock). Topsoil extension into the basement is also largely lateritic but interposed along its course by discrete bodies of sandy clay and to a lesser extent clayey sand. Subgrade composition along the basement axis is characteristically clayey but intermittently occupied by long expanses of laterite.

Table 3. Abridged VES Results over the Basement Complex

VES NUMBER	LAYER NUMBER	RESISTIVITY (Ω m)	THICKNESS (m)	DEPTH (m)	CURVE TYPE	INFERRED LITHOLOGY
18	1	844.2	1.3	1.3	H	Topsoil
	2	48.6	13	14.3		Clay
	3	366.1	---	---		Fractured Basement
19	1	835.5	1.0	1.0	H	Topsoil
	2	36.2	15.0	16.0		Clay
	3	1637.2	---	---		Fresh Basement
20	1	793.6	1.5	1.5	H	Topsoil
	2	79.9	19.6	21.1		Clay
	3	535.0	-	-		Fractured Basement

21	1	493.2	0.9	0.9	KQH	Topsoil
	2	702.9	0.9	1.8		Laterite
	3	440.5	6.7	8.5		Laterite
	4	275.3	56.8	65.3		Clayey Sand
	5	2752.5	-	-		Basement
22	1	263.5	1.2	1.2	KH	Topsoil
	2	746.2	5.9	7.1		Laterite
	3	307.4	42.4	50		Clayey Sand
	4	1570.1	-	-		Fractured Basement
31	1	125.9	0.8	0.8	HAA	Topsoil
	2	77.3	1.8	2.6		Clay
	3	301.6	11.1	13.7		Clayey Sand
	4	388.1	4.5	18.2		Clayey Sand
	5	1607.7	---	---		Fractured Basement
32	1	741.4	0.8	0.8	HA	Topsoil
	2	183.3	2.2	3.0		Sandy Clay
	3	804.1	31.4	34.4		Laterite
	4	2540.8	---	---		Fractured Basement
33	1	164.4	0.8	0.8	HK	Topsoil
	2	71.1	2.0	2.8		Clay
	3	197.7	5.4	8.2		Sandy Clay
	4	43.7	---	---		Clay
34	1	184.5	1.1	1.1	H	Topsoil
	2	31.2	12.7	13.8		Clay
	3	523.4	-	-		Fresh Basement
35	1	459.5	1.0	1.0	KH	Topsoil
	2	557.6	1.0	2.0		Lateritic Clay
	3	26.8	19.6	21.6		Clay
	4	330.5	-	-		Fresh Basement
36	1	243.0	4.5	4.5	H	Topsoil
	2	46.9	24.4	28.9		Clay
	3	673.4	-	-		Fresh Basement
37	1	199.4	0.5	0.5	K	Topsoil
	2	275.1	2.0	2.5		Lateritic Clay
	3	56.2	7.5	10		Clay
	4	852.1	-	-		Fresh Basement
38	1	506	0.9	0.9	H	Topsoil
	2	97.7	5.4	6.3		Clay
	3	1555	-	-		Fresh Basement
39	1	255.5	1.2	1.2	H	Topsoil
	2	112.8	3.4	4.6		Sandy Clay
	3	1221.3	-	-		Fresh Basement
40	4				H	
	1	79.7	0.6	0.6		Topsoil
	2	10.0	3.8	4.4		Clay
	3	1614	-	-		Fresh Basement

Geo-electric Sections and Electrical Resistivity Imagin

Sedimentary Basin Segment

The geo-electric sections from traverse one to four shown in Figures 3 and 4 revealed that the topsoil initially, comprised minor proportion of clay and competent clayey sand occupied a bit further along the road. However, dominantly lateritic soils dominated several kilometres along the road with very minor infusion of clayey sand toward end of the sedimentary section. The underlying stratum beneath the topsoil differs compositionally at various locations. For instance, at Ilisan axis, it extensively composed of sandy clay; with

mainly clay at Irolu. More distinctively, the stratum composed of clayey sand towards the transition. Near this zone, the clayey sand stratum became partly overlain by a lateritic layer which thickens appreciably towards the transition.

Along Ilisan segment, two electro-facies of sandy clay were recognized; namely; the low resistive incompetent upper stratum, and the laterally extensive better resistive fairly competent lower stratum; interposed by incompetent clay bodies towards Irolu. Along Irolu axis, the subgrade largely, composed of clay and underlain by moderately competent clayey sand.

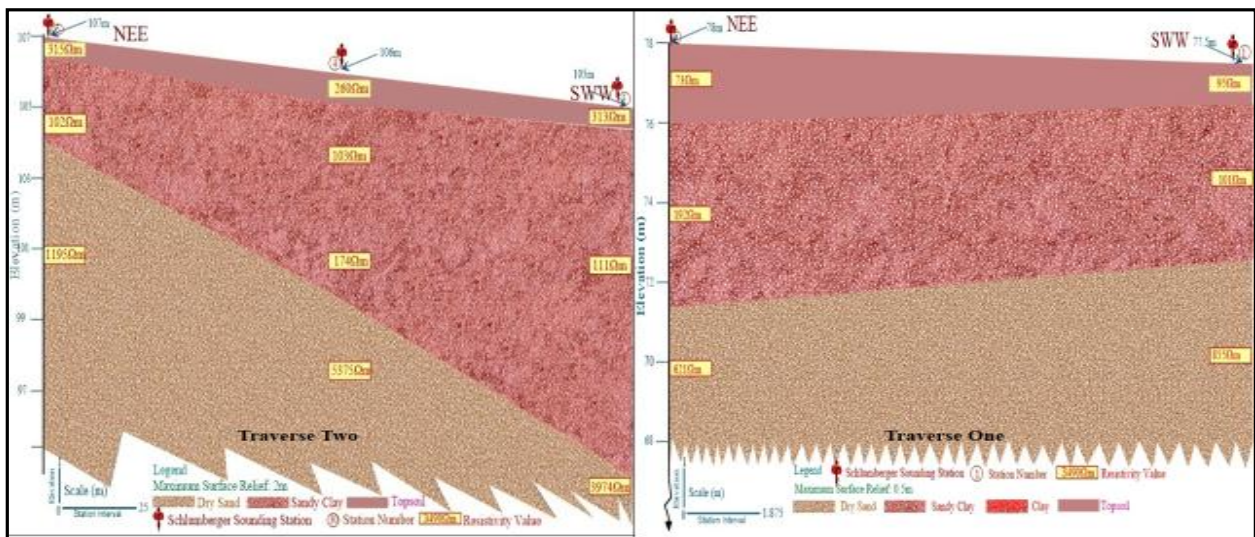


Figure 3. Geo-electric sections for traverses one and two along the sedimentary section

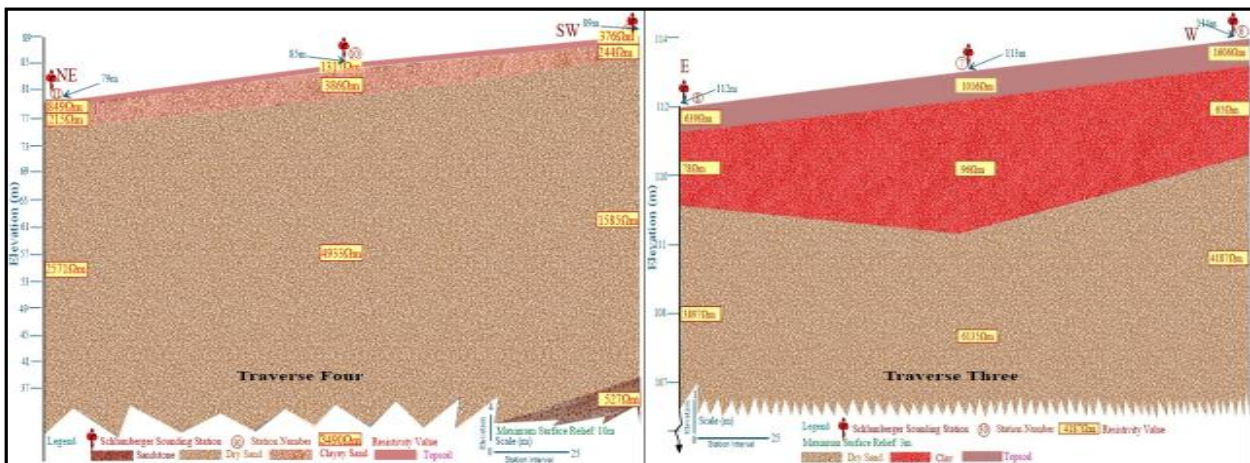


Figure 4. Geo-electric sections for traverses three and four along the sedimentary section

Resistivity distributions along the subgrade's 1st profile shown in Figure 5 ranges from 102 – 421 Ω m; outlining the blue (96- 124 Ω m) colouration as incompetent sandy clay, green (148 - 200 Ω m) as fairly competent sandy clay units and the underlying orange zone (200 - 421 Ω m) also as fairly competent clayey sand unit. Along the 2nd profile, the resistivity contour value of the subgrade ranges from 29–305 Ω m; the blue, green, yellow, red and violet colouration ranges in resistivity value ranges from 29– 50 Ω m, 50- 95 Ω m, 95 - 135 Ω m, 135 – 200 Ω m and 200– 305 Ω m respectively; correspondingly inferred as porous clay, clay, incompetent sandy clay, fairly competent sandy clay and clayey sand. Subgrade resistivity along 3rd profile ranges between 60 – 807 Ω m. Colour blue, green, yellow-red and violet generally exhibit layered resistivity contour pattern on the resistivity structure which from the top to bottom, ranges from 60 - 110 Ω m, 110 – 200 Ω m, 200 – 270 Ω m/270 – 400 Ω m, 400 – 807 Ω m corresponding to clay, sandy clay, clayey sand and sand.

On the inverted resistivity structure along the 4th profile, the blue coloured contours range in resistivity value from 105 – 135 Ω m corresponding to an incompetent sandy clay; green coloured contours (150 - 210 Ω m) occur as discrete lenses of fairly competent material

composed of sandy clay; the lemon-green/yellow coloured contours (210 - 450 Ω m) correspond to an inclined clayey sand stratum that underlies the sandy clay bodies, while also occurring as pockets within the more resistive brown-red/violet (500 - 1300 Ω m) coloured competent sand/dry sand which covers an extensive part of this profile. Contour shades on the resistivity structure along profile 5, from top to base are blue, lemon green and yellow- red-violet. The blue layer ranges in resistivity from 120 - 150 Ω m delineating an incompetent sandy clay unit occurring between distances 96 – 132m.

Resistivity range of lemon-coloured contours is 206 – 398 Ω m indicating a moderately competent clayey sand stratum which stretches through the entire profile though with minor specks of lateritic sand (453-3289 Ω m) interposition. This yellow-red-violet indicated sand layer intercalates at the top completely underlies the clayey sand layer, exhibiting an increasing degree of compaction and competence with depth. In spite the observed disparity within the subgrade, a general recognizable lithological trend composed of clayey earth materials (along Ilisan – Irolu axis) to a better preferred sandy composition (along other part of the sedimentary section) can be assertively deduced from the result.

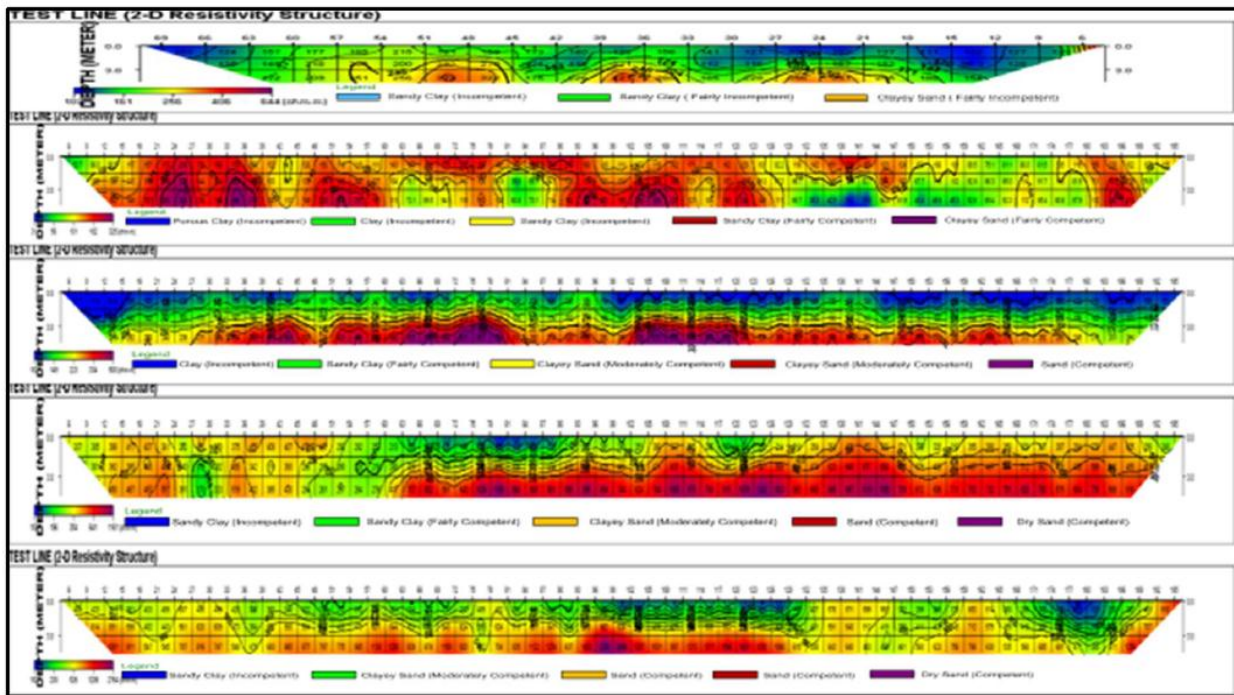


Figure 5. Interpreted inverted tomographical structure along profiles 1 to 5 in the sedimentary segment of the road.

Transition Zone Segment

The delineation of clayey topsoil and the upper sandy clay substratum along Ilisan route as well as inordinate stretch of clay stratum around Irolu is inferentially, deduced as incompetent lithologic units due to their inherent poor permeability property inimical to fluid transmission. Consequentially, fluid invasion of porous clay bodies (especially within the swelling varieties) may occur during water precipitation by rain, and as such dampens the engineering performance of this section of the sedimentary rock-derived subgrade soils.

From Figure 6 the geo-electric sections for traverses five and six along the sedimentary-basement in the transition zone revealed that the lateritic characteristics of the sedimentary rock-derived subgrade soils for the topsoil extends to the transition. This apparently, composed of laterized sand along the

sedimentary margin but abruptly altered to lateritic clay on the basement edge. The subgrade competence is expected to greatly increase spatially from the sedimentary starting point to the contact zone wherein high lithologic heterogeneity was encountered. Constituents of soils in this area include conglomeratic sand, ferruginous sand, sand and ferruginous kaolinite towards the basement section in that order.

Few hundreds of metres away from the transition zone into the basement, the subgrade is largely composed of clay but further along the road constituted by thick lengthy bodies of laterite. Furthermore, progressive basement advancement of the resistivity sounding revealed a subgrade composition constituted by sandy clay and clay. The anticipated severe pavement failure along the basement segment of the road might be cushioned by the approximately 1m thick lateritic topsoil.

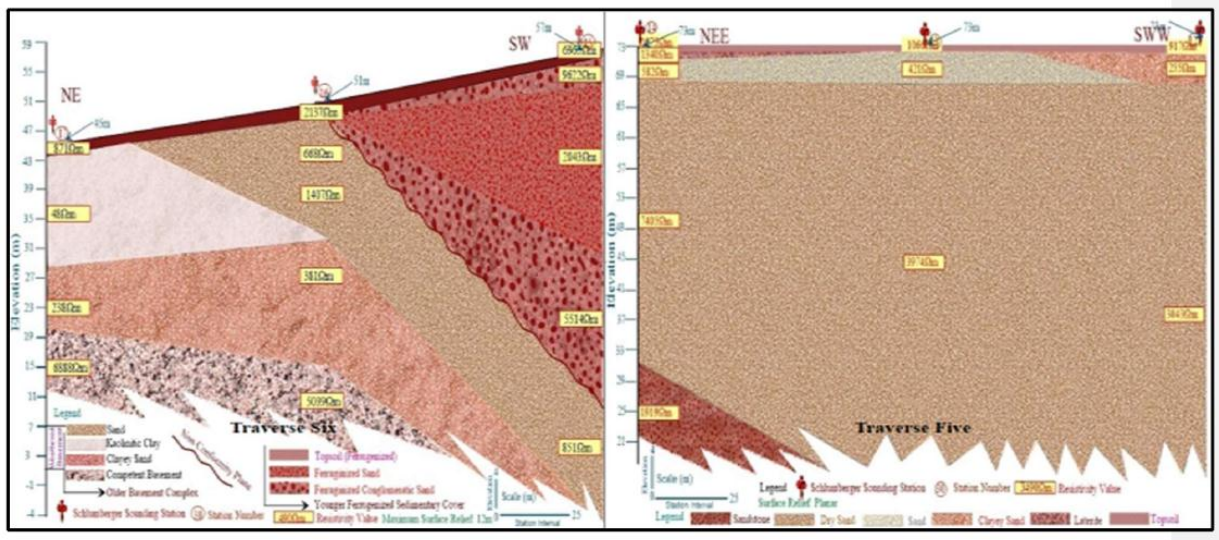


Figure 6. Geo-electric sections for traverses five and six along the sedimentary-basement transition section.

Along this segment, the depicted geo-electric units on the inverted tomographic structure (Figure 7) can be categorized into two, namely; the relatively low resistive blue – green contoured weathered zone and the contrastingly highly resistive yellow-red-violet contoured sedimentary cover. Resistivity – contour blue ranges between 233– 450 Ω m, corresponding to a prominent clayey sand lithology within the weathered layer. The green coloured contour (538– 1008 Ω m) depicts sand along the 6th profile. Sand dominates the upper portion of the weathered layer but spatially occurs as discontinuous lenses within the highly resistive lateritic sand along the sedimentary boundary. However, along the 7th profile, an irregularly inclined yellow shaded contour (1473- 2514 Ω m) marks the non-conformity structure. In other areas, contour yellow also indicates sand units. Red contour shades exhibit a resistivity range between 3289 - 8028 Ω m; correspondingly inferred as lateritic sand. The violet-coloured resistivity contours possess a resistivity >3289 Ω m - inferred as a dry sand layer, underlying the reddish lateritic sand.

This geologic model towards the basement revealed fractured locations, other layered boundaries and unconformable zones. From structural perspective, unconformities are stratigraphic discontinuities (Bayewu *et al.*, 2011). Olorunfemi *et al.*, (2004) explained that this is undesirable for road pavement construction. It is therefore, necessary to put good road architecture into consideration in the course of the lithologic disparity of the subgrade soils along the road. This will enable the avoidance differential response to wheel load, and enhance better engineering performance.

Beyond Ilisan – Irolu segment to the transition boundary, the subgrade is largely constituted by stable heterogeneous engineering materials of varying degree of competence. Bulk of which are sandy facies (ferruginous sand, ferruginous conglomeratic sand, sand and clayey sand) but chiefly clay-dominated (kaolin) on the basement margin of the unconformity which is a major source of geologic concern.

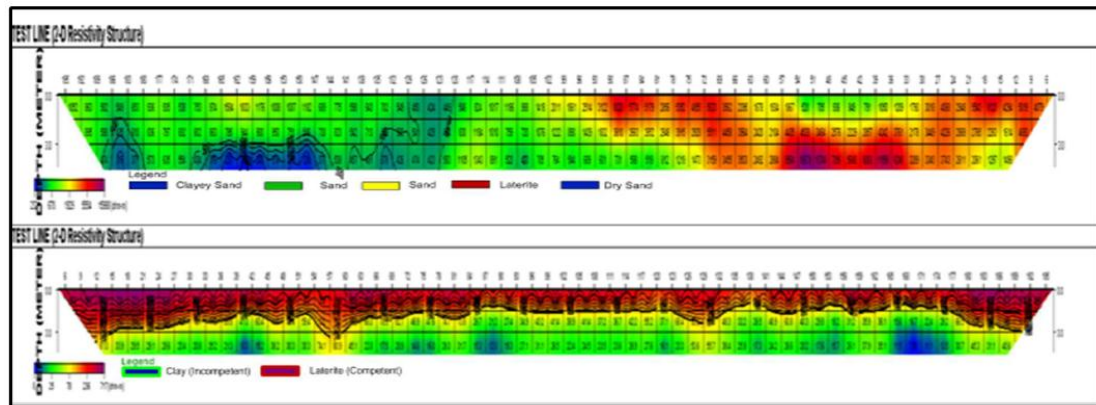


Figure 7. Interpreted inverted tomographical structure along profiles 6 and 7 in the transition zone segment of the road.

From the transition zone to the basement area, antithetical occurrence of geological structures beneath the route may further directly or indirectly reduce the engineering performance of the subgrade (Olorunfemi *et al.*, 2004). Fractures and unconformity are two peculiar discontinuities encountered along the basement and transition segment of the highway respectively. Unlike faulting, non-conformity creates an immovable structural gap between a crystalline terrain and sedimentary basin, which if well reinforced would have very limited destabilizing effect on the subgrade (Bayewu *et al.*, 2011). Advancing from the transition zone to the basement area as shown in traverse 6, revealed an upper lateritic layer underlain by clay along the first sub segment. The laterite dominated subgrade along the next sub segment. This is followed by a heterogeneous subgrade dominated by sandy clay –overlain to a certain by laterite but underlain beneath by relatively minor lenses of clay along the third the sub segment. Next is a partly lateritic subgrade co-occurring with clay and sandy clay along the fourth sub segment and assorted mix of clay, sandy clay, clayey sand with sand along the fifth and sixth sub-segment.

Basement Complex Segment

The geo-electric sections from traverses seven to twelve (Figures 8-10) along the Basement Complex section of the road revealed that the topsoil extension into the basement is largely lateritic. This is interposed along its course by discrete bodies of sandy clay, and to a lesser extent clayey sand. The subgrade composition along road in the area underlain by the Basement Complex axis is characteristically clayey. However, it is intermittently occupied by long expanses of lateritic soils. There is a very high tendency for incessant failure along the unstable heterogeneous basement subgrade, minimal along the transition and might be expectedly stable along sedimentary segment.

Majority of the basement fractures are deeply seated, and as such may poses no threat to subgrade except when relative block movement occurs. The latter scenario may arise along the fault plane of traverse 10 (Figure 9) where suspected easterly displacement of the hanging wall is perceptible on the normal faulted block.

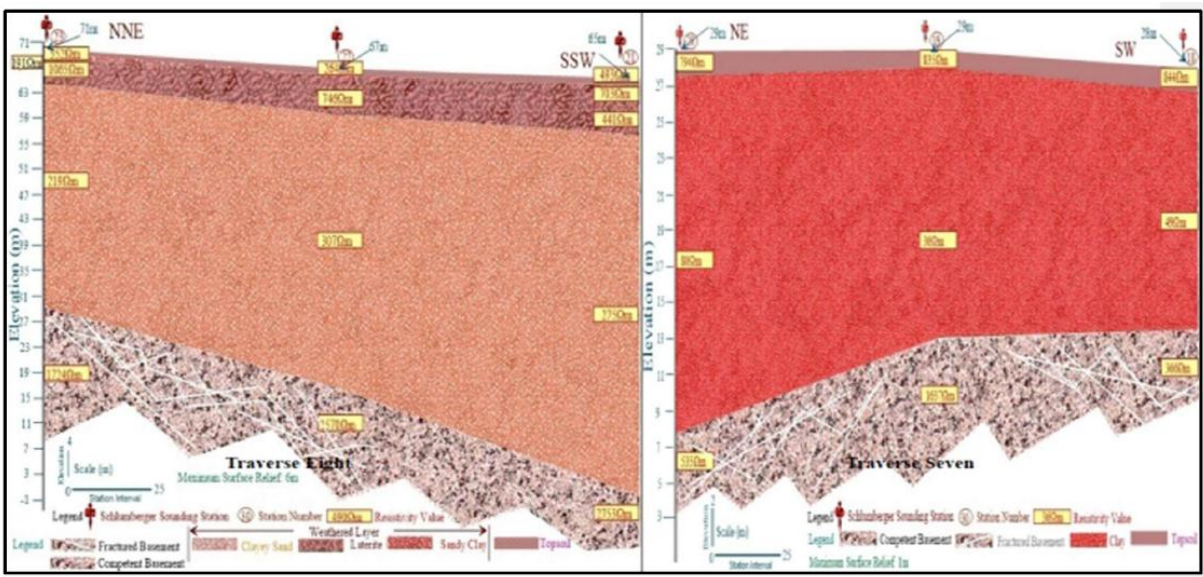


Figure 8. Geo-electric sections for traverses seven and eight along the basement section.

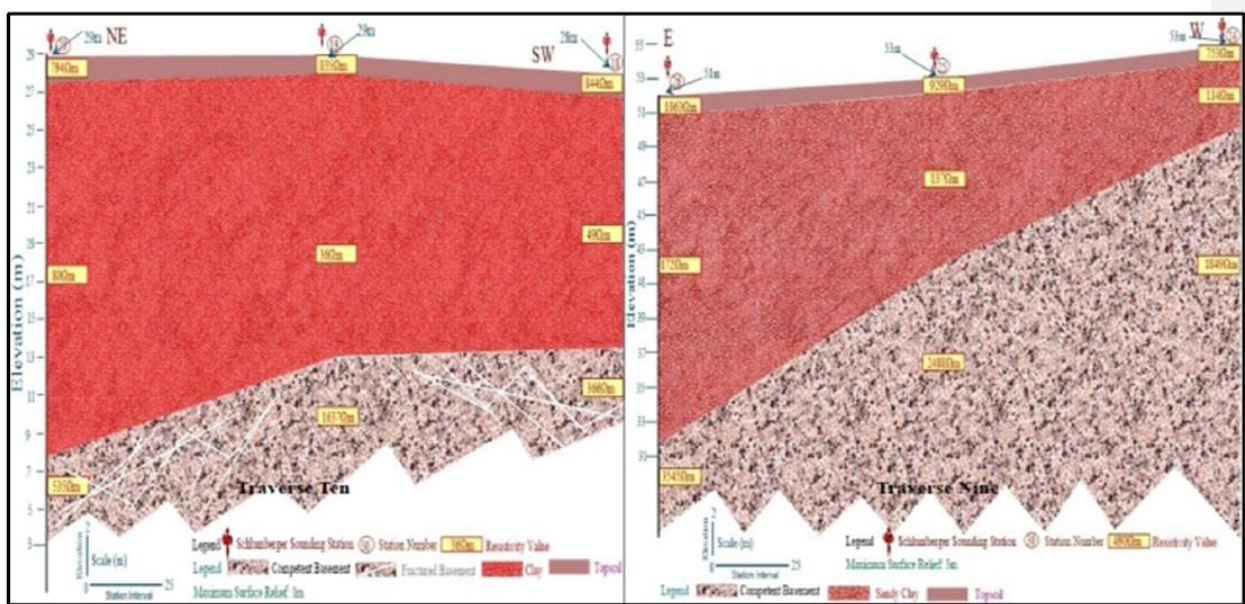


Figure 9. Geo-electric sections for traverses nine and ten along the basement section.

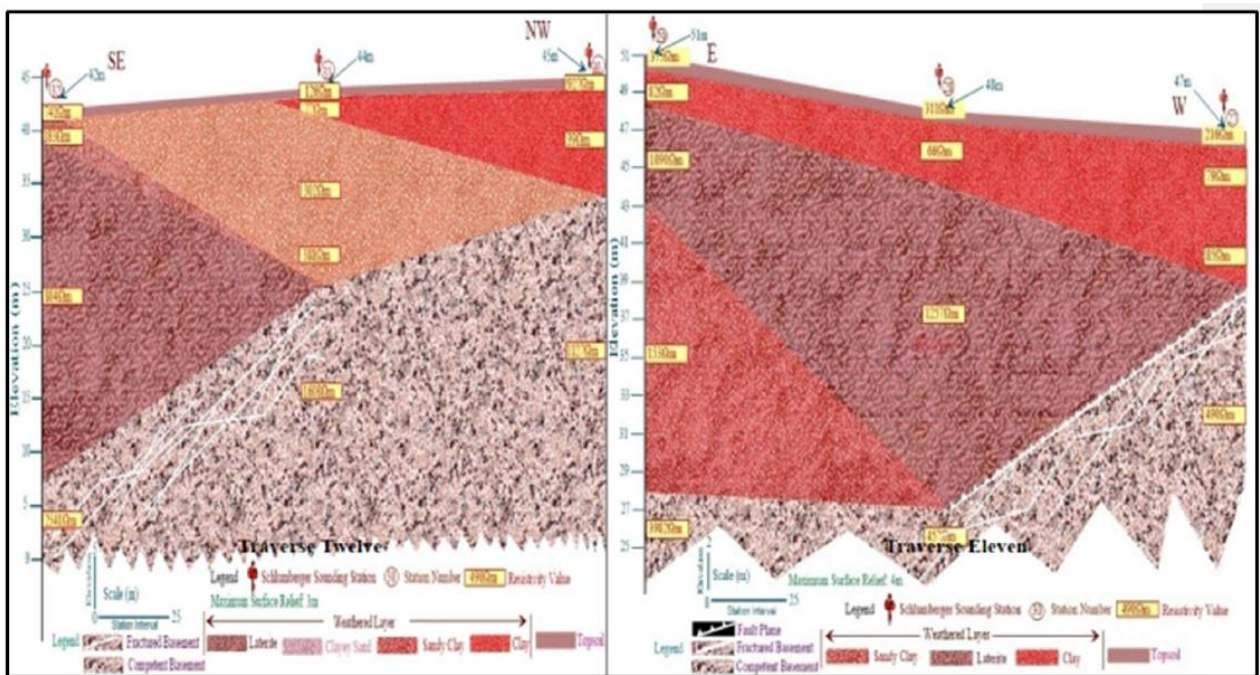


Figure 10. Geo-electric sections for traverses eleven and twelve along the basement section.

Crystalline rocks disintegration differs at various rates under same climatic condition due to petrologic variation. The composition and relative abundance of the various clayey minerals in the weathered products affect the mechanical properties of the subgrade. The weathered Subgrade setting, as revealed on the resistivity structure in Figure 11 along profile 8, depicts two main contrasting layered resistivity zones which from top to base range between 300 - 721 Ω m and 8 - 83 Ω m, corresponding to an lateritic layer and a lower clay layer infused with pockets of porous clay at distance ranges of 39– 45m, 72 – 78m, 84 – 90m, 120m – 125m, 138m – 141m, 150m – 156m and 165m – 177m. Pavement failure is imminent along this section due to proximity of the clay layer to the surface and the unwanted presence of the unstable porous clay lenses within this layer. Moreover, if the delineated underlying layer does not settle differentially, the observed surface stability could be preserved.

The inverted resistivity structure along segment (profile 9) revealed two prominent

competent resistivity units ranging between 580- 3009 Ω m (red –violet) and 237 - 555 Ω m (green – lemon) within which a very insignificant incorporation of a fairly competent unit (160 - 210 Ω m) occurs; inferred subgrade materials in aforementioned order are laterite, clayey sand/sand and sandy clay lenses. Stability of the subgrade can be generally rated as being moderate, as greater proportion of the subgrade is composed of moderately competent to competent laterite with relatively minor proportion of fairly competent sandy clay, clayey sand and sand. Durable pavement can be securely constructed along this road segment. Inversion model envisioned along segment 9 is marked by resistivity heterogeneity ranging from 784 Ω m - 1210 Ω m (red-violet), 250 - 500 Ω m (yellow), 122 - 212 Ω m (lemon green) and <100 Ω m (blue); inferred as lateritic sand, lateritic clay, sandy clay and clay. By the virtue of the undesired heterogeneous composition of this subgrade section, high failure severity is anticipated, more particularly, directly over the clay pockets as these bodies settle(sag)

differentially within the adjoining subgrade materials. This observed heterogeneity further extends to the 10th profile, which on its resistivity structure depicts contrasting zones of high(400 - 800 Ω m), moderate (201 - 275 Ω m) and lows (45 - 97 Ω m) resistivity; delineated as heterogeneous mix of laterite (red - violet), clayey sand (yellow) and clay (blue). Pavement failure, as envisaged, would be preponderated within the central portion of this segment - underlain by incompetent subgrade materials (sandy and clay).

Advance investigation into the basement (profile 11) continuously projects an extension

of the erratic heterogeneous character of the basement subgrade; spatially comprising of laterite (600 - 1555 Ω m), clay/porous clay (52 - 85 Ω m/21 - 42 Ω m) and clayey sand(197 - 258 Ω m). It is therefore unsurprising to observe a laterally extensive failed segment directly over the clay constituted sections. Electrical resistivity structure from the final survey (profile 12), revealed two resistivity units whose ranges are 45- 86 Ω m (lemon green), and 244 - 569 Ω m (red) inferred as clay and lateritic clay. Failure is imminent, but was not noticeable along this axis.

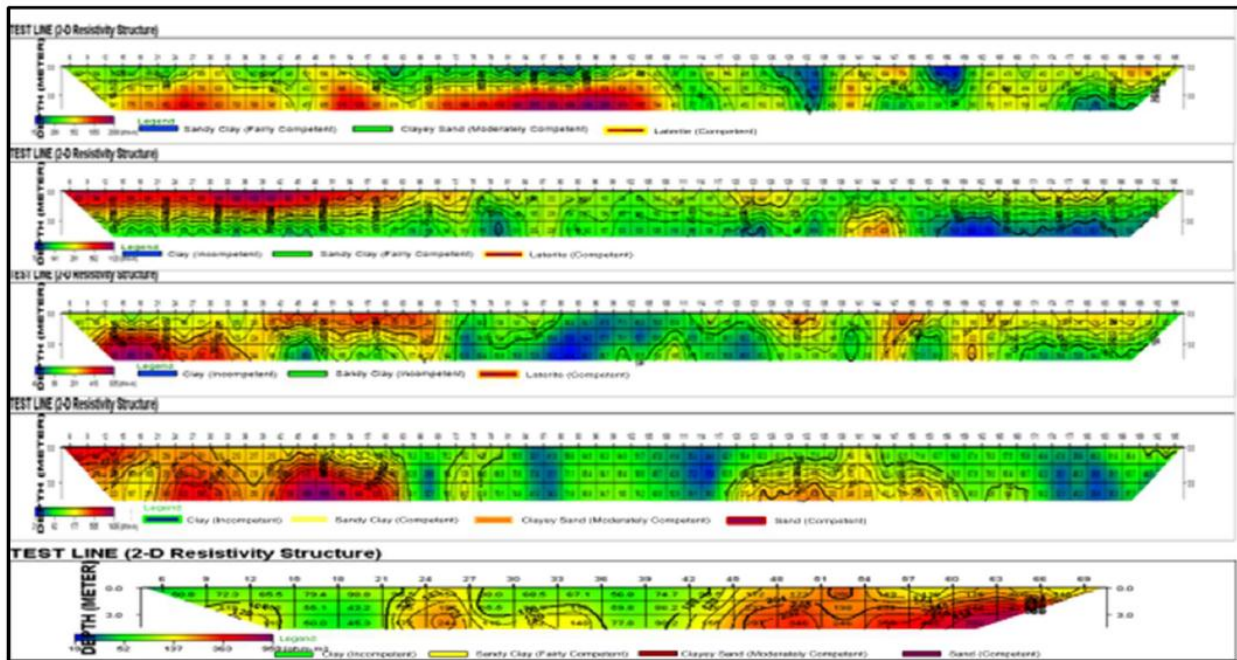


Figure 5. Interpreted inverted tomographical structure along profiles 8 to 12 in the basement complex segment of the road

CONCLUSION AND RECOMMENDATIONS

The electrical resistivity method was used as a geotechnical geophysical tool to image, and characterize the shallow subsurface which underlain the Ago-Iwoye/Ilishan road. This measured specific parameters that revealed bedrock depth, rock type, layer boundaries, weak zones, likely expansive clays, and fractures. The field reconnaissance inspection

confirmed the two major geological environments across the entire stretch of the road was via existing and newly adjoined accessibility; the Precambrian Basement Complex, and Ise Formation in the Dahomey (Sedimentary) Basin.

Geo-electric layers revealed that the road is underlain by Sedimentary Formation of the Dahomey Basin between Ilishan and Irolu. At Irolu, the road is underlain by the termination

of the Sedimentary Basin as inferred from anomalously high resistivity. Between Irolu and Ijesha-Ijebu, anomalous by ferruginous conglomeratic sandstone. At Ijesha-Ijebu, the road is underlain by abrupt contrast along the plane of an unconformity (non-conformity). An apparent lithologic overlap between sedimentary to basement boundary indicative of a Transition Zone, is evident from the geoelectric layers obtained between the Sedimentary Basin and the Basement Complex terrains. The resulting layering parameters along the basement segment revealed a range of three (3) to five (5) geoelectric layers. The lithologic inferences are the topsoil, capped or uncapped heterogeneous weathered unit of sand, kaolinitic clay, clayey sand and the fractured/fresh bedrock.

The 2-D resistivity structures across the different geological terrains revealed a broad range of resistivity values from the Sedimentary Basin (50 - 3289 Ω m), Transition Zone (233 - 8028 Ω m) and the Basement Complex (8 - 3009 Ω m) subgrade soils. There is occurrence of laterite layer across the entire three segments although, greater abundance is of laterite occurs in the Basement Complex terrain. From geotechnical point of view, vast proportion of the subgrade materials underlying the Sedimentary Basin and Transitional Zone segments can be adjudged competent due to sand and clayey sand units with minor occurrences of incompetent clay and sandy clay lenses. The occurrence of subsurface discontinuities (fault and non-conformity) along the Basement –Sedimentary interface (Transitional Zone) of the road would also adversely affect the pavement stability. Areas where the road is underlain by fracture, fault and other lithological contact should be grouted by cement.

The setting encountered along the Basement Complex segment is characterized by high

preponderance of clay and sandy clay units with minor proportion of sand within the subgrade. More serious failure of the road is imminent in this segment, due to incompetent clayey subgrade soils. Replacement of subgrade soils at the location underlain by Basement Complex rocks, with a high-quality construction aggregate. This is expected to provide the required stability and durability of the pavement as well as prevent potential road failure and other associated risks. The diverse geologic environment must be taken into consideration in the course of its rehabilitation. Construction of drainage channels at both sides of the road pavement especially, where road pavement runs parallel to runoff precipitating high relief is strongly recommended. This geophysical application does not substitute for boring and geotechnical testing however, it has reliably revealed the image of the subsurface for predicting the engineering performance of the subgrade soils.

REFERENCES

- Adebisi, N. O. and Fatoba, J. O. (2013). Instrumentation for *In-situ* Foundation Investigation in Lagos, South West (SW) Nigeria. *Journal of Geology and Mining Research*. 5 (4), pp. 88-96.
<http://www.academicjournals.org/JGMRIndia>
- Anderson, N. L. (2006) Selection of Appropriate Geophysical Techniques: A Generalized Protocol Based on Engineering Objectives and Site Characteristics. *Proceeding of the Highway Geophysics-NDE Conference*, pp. 29–47. Available at <http://2006geophysics.mst.edu/>
- Anderson, N., Croxton, N., Hoover, R. and Sirles, P. (2008) *Geophysical Methods Commonly Employed for Geotechnical Site Characterization*. Transportation Research Circular e-c130 ISSN 0097-8515

- Akanni, C.O. (1992). Aspect of climate. In Ogun state in maps. Edited by Oyesiku, K. & Jegede, J. Rex Charles publ. pp.18-19.
- Balogun, B. O. (2019). Tectonic and structural analysis of the Migmatite–Gneiss–Quartzite complex of Ilorin area from aeromagnetic data. *Nigerian Journal of Astrology and Geophysics*. 8 (1), pp. 22-33.
- Bayewu, O. O., Oloruntola, M. O. and Mosuro, G.O. (2011) Application of electrical resistivity imaging (ERI) in delineating a non-conformity around Ijesha-Ijebu, southwestern Nigeria *Journal of Petroleum and Gas Exploration Research* (ISSN 2276-6510), 2(1) 010-016.
- Capozzoli, L., and Rizzo, E. (2017) Virtual Special Issue Ground-Penetrating Radar and Complementary Non-Destructive Testing Techniques in Civil Engineering Combined NDT techniques in civil engineering applications: Laboratory and real test. *Journal of Construction and Building Materials*, 154, 1139-1150.
- Coe, J. F., Mahvelati, S. and Asabere, P. K. (2017) *Application of Nondestructive Testing and Geophysical Methods to Evaluate Unknown Foundation Geometry*. Proceeding of the 29th Central Pennsylvania Geotechnical Conference Hershey, Pennsylvania.
- Hempen, G. L., and D. L. Butler. (2000) Contracting for Geophysical Services. *Proc., Geophysics 2000, The First International Conference on the Application of Geophysical Methodologies and NDT to Transportation Facilities and Infrastructure*. Missouri Department of Transportation and FHWA, 2000.
- Hoover, R. A. (2004) Evolving Geophysical Standards. *Proc., Symposium on the Application of Geophysics to Environmental and Engineering Problems*, Environmental and Engineering Geophysical Society, 2005. Available at www.eegs.org.
- Karous, M.R. and Hjelt, S.E. (1983). Linear filtering of VLF Dip Angle Measurements. *Geophysical Prospecting*, 31, pp. 782-794.
- Martinho, E. and Dionísio, A. (2014) Main geophysical techniques used for non-destructive evaluation in cultural built heritage: A review. *Journal of Geophysics and Engineering*. 11(5):053001,15. DOI: 10.1088/1742-2132/11/5/053001
- N.G.S.A. (2006) *Geological and Mineral Resources Map of Cross River State, Nigeria*. A publication of the Nigerian Geological Survey Agency,
- Olayinka, I. A. and Oyedele, K. F. (2001) Geoelectrical survey in site investigation of locations along Ibadan-Ilorin dual carriageway. *Journal of Mining and Geology*. 37, pp. 163-175
- Oli, I. C., Okeke, O. C., Abiahu, C. M. G., Anifowose, F. A., and Fagorite, V. I. (2019) A Review of the Geology and Mineral Resources of Dahomey Basin, South-western Nigeria. *International Journal of Environmental Sciences and Natural Resources*. 21 (1), 036 – 040 DOI: 10.19080/IJESNR.2019.21.556055
- Olorunfemi, M. O, Idornigie, A. I, Coker, A.T, Babadiya, G.E. (2004). On the application of the electrical resistivity method in foundation failure investigation – A case study. *Global Journal of Geological Sciences*, 2 (1), 139–151.
- Scalenghe, R., Territo, C., Petit, S., Terribile, F., Righi, D. (2016). The role of pedogenic overprinting in the obliteration of parent material in some polygenetic landscapes of Sicily (Italy). *Geoderma*

- Regional*. 7: pp. 49–58. doi:10.1016/j.geodrs.2016.01.003
- Sirles, P. C. (2006). *NCHRP Synthesis 357: Use of Geophysics for Transportation Projects*, Transportation Research Board of the National Academies, Washington, D.C., Available at http://onlinepubs.trb.org/onlinepubs/nchrp/nchrp_syn_357.pdf.
- Transportation Research Circular (TRC, 2008) Geophysical Methods Commonly Employed for Geotechnical Site Characterization. E-C-130. ISSN 0097-8515
- Wightman, W. E., F. Jalinoos, P. Sirles, and K. Hanna (2004). *Application of Geophysical Methods to Highway-Related Problems*. Publication No. FHWA-IF-04-021. Central Federal Lands Highway Division, FHWA, U.S. Department of Transportation, Available at www.cflhd.gov/agm/index.htm